Environmental Fluid Mechanics (2022) 22:1233–1252
https://doi.org/10.1007/s10652-022-09888-9

ORIGINAL ARTICLE

Effect of anisotropy and boundary conditions on Darcy and Brinkman porous penetrative convection

Brian Straughan[1]

Received: 11 April 2022 / Accepted: 5 July 2022 / Published online: 17 August 2022

Abstract

We investigate the effects of anisotropic permeability and changing boundary conditions upon the onset of penetrative convection in a porous medium of Darcy type and of Brinkman type. Attention is focussed on the critical eigenfunctions which show how many convection cells will be found in the porous layer. The number of cells is shown to depend critically upon the ratio of vertical to horizontal permeability, upon the Brinkman coefficient, and upon the upper boundary condition for the velocity which may be of Dirichlet type or constant pressure. The critical Rayleigh numbers and wave numbers are determined, and it is shown how an unconditional threshold for nonlinear stability may be derived.

Highlights

- Shows how number of convection cells depends upon the temperature of the upperlayer and the anisotropy of the permeability
- Shows how number of convection ceels depends upon the temperature of the upperlayer and the Brinkman coefficient
- Shows how number of convection cells patters depends upon the upper boundarycondition on the velocity or the ambient pressure

Keywords Penetrative convection · Anisotropy · Boundary conditions · Darcy porous media · Brinkman porous media

1 Introduction

Penetrative convection is a phenomenon whereby thermal convection may commence in a sub-layer of a horizontal layer of fluid, or in a horizontal layer of fluid saturated porous medium, and the ensuing convective motion will induce motion in other part(s) of the layer. It typically induces counter rotating convection cells. Mathematical models for penetrative

✉ Brian Straughan
brian.straughan@durham.ac.uk

[1] Department of Mathematical Sciences, University of Durham, Stockton Road, Durham DH1 3LE, UK

convection typically involve either a quadratic density in the buoyancy force or an internal heat source, see e.g. Straughan [1, pages 97–102]. We here concentrate on the model where density is a quadratic function of temperature, as introduced by Veronis [2], for the case of a layer of incompressible viscous fluid.

The fact that penetrative convection is of such interest is primarily due to the realization that it is an area with a multitude of real physical applications. As pointed out in Straughan [1], there are applications in planetary physics, DietrichWicht [3], van den berg et al. [4], in internally cooled convection,Berlengiero et al. [5], in environmental fluid mechanics, Fernando [6],Pol and Fernando [7], in the cloud cover of Venus, Imamura et al. [8], in aiding the rise of volcanic plumes in the Earth's atmosphere, Kaminski et al. [9], in mixing in the Laptev Sea, Kirillov et al. [10], in cloud to ground discharges,Machado et al. [11], Mharzi et al. [12], in biochemical decay,Prudhomme and Jasmin [13], in flow in the Sun, Tikhomolov [14], and in particular in penetrative convection in a porous medium where application is to formation of stones into regular patterns, George et al. [15], and in building insulation, Straughan and Walker [16]. Theoretical analyses of penetrative convection have ensued such as Veronis [2], Musman [17], Carr [18, 19], Carr and Putter [20], Carr and Straughan [21], Harfash [22, 23], Krishnamurti [24], Larson [25], Straughan [26–28]. Further references may be found in the books of Straughan [29, 30].

DietrichWicht [3] write,..."*Many celestial objects are thought to host interfaces between convective and stable stratified interior regions. The interaction between both, e.g. the transfer of heat, mass, or angular momentum depends on whether and how flows penetrate into the stable layer. Powered from the unstable, convective regions, radial flows can pierce into the stable region depending on their inertia (overshooting)*. Veronis [2] developed and analysed a model for penetrative convection in an infinite horizontal layer of water where the temperature at the bottom of the layer is kept fixed at 0 °C while the temperature of the upper plane is kept fixed at temperature $T_U(\geq 4\ °C)$. Water possesses a density maximum at approximately 4 °C and thus the Veronis [2] situation has water in the 0 °C to 4 °C range in a potentially gravitationally unstable configuration. When convective motion commences it can penetrate into the part of the layer where the temperature is above 4 °C, and if the upper temperature is sufficiently high then a second counter rotating fluid cell may arise in the upper part of the layer, see e.g. the streamlines shown in Musman [17]. In this article we are interested in finding critical Rayleigh numbers and wave numbers for when penetrative convection may occur in a porous medium saturated with water where the geometric configuration is the Veronis [2] one, i.e. the lower boundary temperature held at 0 °C with the upper temperature fixed at T_U. Of particular interest to us is to determine the conditions under which one convection cell occurs, and when two or more will occur. Since we are employing a porous medium we have several influences to consider, such as whether the porous medium is isotropic or anisotropic, what conditions are imposed on the fluid at the upper boundary, and what theory is employed to describe the porous medium, e.g. Darcy theory or Brinkman theory. Flow patterns in the porous medium are important in transporting micro particles or contaminants which may subsequently be distributed into the surrounding environment where they may degrade quantities such as air quality. Therefore, an understanding of the flow patterns in saturated porous media due to penetrative motions is essential for a complete knowledge of the physics of the environment.

The goal of this work is to analyse models for penetrative convection in a porous material of Darcy or Brinkman type allowing for the porous structure to be of horizontally isotropic type. We consider a fixed boundary condition for the fluid at the upper boundary of the layer but alternatively we allow a condition of constant pressure. We derive critical Rayleigh numbers and wave numbers for the onset of penetrative convection and investigate in detail the conditions on the upper boundary temperature which give rise to a single convection cell or multiple cells. This is achieved by finding the associated eigenfunctions of the instability problem and our results vary strongly depending on the degree of anisotropy, the upper boundary condition on the velocity, or which porous medium theeory is utilized.

2 Equations for penetrative convection

Suppose the porous medium occupies the horizontal layer $\mathbb{R}^2 \times \{z \in (0,d)\}$ with gravity g acting in the downward direction, i.e. $g_i = -gk_i$, where $\mathbf{k} = (0,0,1)$. The lower plane $z = 0$ is held at fixed temperature 0 °C while the upper plane at $z = d$ is held at fixed temperature $T_U \geq 4$ °C.

For a linear density–temperature relationship the governing equations for an isotropic Darcy porous medium are given by Straughan [30] in equations (4.1), p. 148, and we repeat these here but we allow for a density which is quadratic in temperature T. Thus, the governing equations are

$$\begin{aligned} 0 &= -\frac{\mu}{K} v_i - p_{,i} - \rho(T) g k_i, \\ v_{i,i} &= 0, \\ T_{,t} + v_i T_{,i} &= \kappa \Delta T, \end{aligned} \tag{1}$$

where the density ρ is given by

$$\rho(T) = \rho_0 (1 - \alpha [T-4]^2), \tag{2}$$

with ρ_0 the density of water at 4 °C and where α is the coefficient of thermal expansion. In (1) v_i, μ, K, p, g and κ are the velocity field, the dynamic viscosity of water, the permeability of the porous material, the pressure of the water in the saturated porous medium, gravity, and the thermal diffusivity of the porous medium. Standard indicial notation is used throughout in conjunction with the Einstein summation convention, so that for example, if $\mathbf{v} = (v_1, v_2, v_3) \equiv (u, v, w)$ and $\mathbf{x} = (x_1, x_2, x_3) \equiv (x, y, z)$, then we write the divergence of the velocity field in the forms

$$\begin{aligned} v_{i,i} \equiv \sum_{i=1}^{3} v_{i,i} &= \frac{\partial v_1}{\partial x_1} + \frac{\partial v_2}{\partial x_2} + \frac{\partial v_3}{\partial x_3}, \\ &= \frac{\partial u}{\partial x} + \frac{\partial v}{\partial y} + \frac{\partial w}{\partial z}. \end{aligned}$$

For an example involving a nonlinearity, we write

$$v_i T_{,i} \equiv \sum_{i=1}^{3} v_i T_{,i} = u\frac{\partial T}{\partial x} + v\frac{\partial T}{\partial y} + w\frac{\partial T}{\partial z}.$$

Many porous materials display distinct anisotropy in their structure and this may be manifest by replacing the scalar permeability K with a tensor K_{ij}. In this case the relevant equations are

$$
\begin{aligned}
0 &= -\mu v_i - K_{ij} p_{,j} - \rho(T) g K_{ij} k_j, \\
v_{i,i} &= 0, \\
T_{,t} + v_i T_{,i} &= \kappa \Delta T,
\end{aligned}
\tag{3}
$$

cf. Straughan [30, page 149].

If we consider an isotropic Brinkman theory then the equations are

$$
\begin{aligned}
0 &= -\frac{\mu}{K} v_i - p_{,i} + \tilde{\mu} \Delta v_i - \rho(T) g k_i, \\
v_{i,i} &= 0, \\
T_{,t} + v_i T_{,i} &= \kappa \Delta T,
\end{aligned}
\tag{4}
$$

where $\tilde{\mu}$ is a Brinkman effective viscosity, cf. Straughan [30, page 150].

The boundary conditions we consider in this article are

$$
T = 0\,^\circ\mathrm{C} \text{ at } z = 0; \quad T = T_U \text{ at } z = d; \quad W = 0 \text{ at } z = 0, \tag{5}
$$

and either

$$
W = 0 \text{ at } z = d, \tag{6}
$$

or

$$
p = p_a \text{ at } z = d, \tag{7}
$$

where p_a is a constant ambient surface pressure.

The steady temperature field for all cases is

$$
\bar{T} = \beta z, \tag{8}
$$

where $\beta = T_U / d$. The steady velocity field in whose stability we are interested is

$$
\bar{W} \equiv 0. \tag{9}
$$

3 Effects on penetrative convection

Our main concern here is to investigate the effect of anisotropy via K_{ij}, the changes due to the Brinkman term with coefficient $\tilde{\mu}$, and the effect of the boundary conditions (6) or (7), upon the critical parameters of penetrative convection.

Anisotropic effects upon thermal convection in saturated porous media have been the subject of many recent investigations, see e.g. Capone et al. [31–35], Hemanthkumar et al. [36–38]. In particular the ramifications of anisotropy in porous media have proved of interest in the application to healthcare materials and in human tissues, see Fang et al. [39], Mirbod et al. [40].

The Brinkman effect upon thermal convection in porous media has also inspired recent research such as Rees [41], Gentile and Straughan [28, 42] and Wu and Mirbod [43]. Of particular note is the observation by Wu and Mirbod [43] that μ and $\tilde{\mu}$ in $(4)_1$ will *not* in general be the same. In [28] it is also shown that the Darcy theory in equations (1) and the Brinkman theory in (4) can lead to very different physical effects and thus the two theories should always be considered separately.

The influence of non-Dirichlet boundary conditions on either the velocity field or the temperature field is also an area which has attracted much recent attention in thermal convection in porous media, see e.g. Barletta et al. [44], Barletta [45], Barletta [46], Barletta and Celli [47], Barletta and Rees [48], Celli and Kuznetsov [49], Mohammad and Rees [50], Nield and Kuznetsov [51], Rees and Barletta [52], Rees and Mojtabi [53, 54], Brandao et al. [55].

In order to place the mathematical theories of flow in porous media on a firm mathematical footing there have been many recent articles studying structural stability aspects of the equations themselves, see e.g. Li et al. [56],Liu and Xiao [57], Liu et al. [58], Liu et al. [59], Liu et al. [60],Gentile and Straughan [61].

We next investigate instability of the basic solution (8), (9), under variation of the effects of anisotropy, the Brinkman coefficient, boundary conditions, and the upper temperature T_U.

4 Instability

To investigate instability of the conduction solution (8), (9), we introduce perturbations u_i, π, θ to v_i, p, T as

$$v_i = \bar{v}_i + u_i, \quad p = \bar{p} + \pi, \quad T = \bar{T} + \theta,$$

and we then non-dimensionalize with the scales given in George et al. [15] and Straughan [37]. The scalings needed are

$$\begin{aligned} &u_i = u_i^* U, \qquad \theta = \theta^* T^\sharp, \qquad x_i = x_i^* d, \qquad t = t^* \mathcal{T}, \\ &\mathcal{T} = \frac{d^2 \rho_0}{\mu}, \qquad U = \frac{\mu}{\rho_0 d}, \qquad P = \frac{\mu U d}{K} \qquad T^\sharp = U \Big[\frac{\beta d^2 \mu}{\kappa \rho_0 g \alpha (T_U - T_L) K} \Big]^{1/2}, \end{aligned}$$

with K replaced by K_H in the anisotropic permeability case. This yields the non-dimensional perturbation equations for (1) as

$$\begin{aligned} &0 = -\pi_{,i} - u_i - 2R\theta(\xi - z)k_i + Pr\theta^2 k_i, \\ &u_{i,i} = 0, \\ &Pr(\theta_{,t} + u_i \theta_{,i}) = -Rw + \Delta\theta, \end{aligned} \tag{10}$$

where the domain is $\mathbb{R}^2 \times \{z \in (0,1)\} \times \{t > 0\}$, $Pr = \mu/\kappa\rho_0$ is the Prandtl number, $\xi = (T_0 - T_L)/(T_U - T_L)$, $T_0 = 4\,°\mathrm{C}$, $T_L = 0\,°\mathrm{C}$, and R is defined by

$$R^2 = \frac{g\alpha\rho_0\beta^2 d^3 K}{\kappa\mu}. \tag{11}$$

When dealing with the Darcy models we present results in terms of a Rayleigh number

$$Ra = \xi^3 R^2, \tag{12}$$

which reflects the depth of the destabilizing layer in the steady state, cf. George et al. [15].

For the Darcy anisotropic case we suppose the permeability tensor is that appropriate to horizontal isotropy so that $K_{ij} \equiv diag\{K_H, K_H, K_V\}$ cf. Straughan [37]. Then with $\ell^2 = K_H/K_V$ the non-dimensional perturbation equations are

$$
\begin{aligned}
&0 = -\pi_{,i} - D_{ij}u_j - 2R\theta(\xi - z)k_i + Pr\theta^2 k_i,\\
&u_{i,i} = 0,\\
&Pr(\theta_{,t} + u_i\theta_{,i}) = -Rw + \Delta\theta,
\end{aligned}
\tag{13}
$$

which are again defined on the domain $\mathbb{R}^2 \times \{z \in (0,1)\} \times \{t > 0\}$, and where $D_{ij} \equiv diag\{1, 1, \ell^2\}$, and now $R^2 = g\alpha\rho_0\beta^2 d^3 K_H/\kappa\mu$. It is worth observing that Straughan [37] provides many instances of real geophysical situations where the horizontally isotropic form D_{ij} is valid.

For the Brinkman system (4), a form of the non-dimensional perturbation equations which incorporates a horizontally isotropic permeability is

$$
\begin{aligned}
&0 = -\pi_{,i} - D_{ij}u_j + B\Delta u_i - 2R\theta(\xi - z)k_i + Pr\theta^2 k_i,\\
&u_{i,i} = 0,\\
&Pr(\theta_{,t} + u_i\theta_{,i}) = -Rw + \Delta\theta,
\end{aligned}
\tag{14}
$$

where $B = \tilde{\mu}K_H/\mu d^2$ is a non-dimensional form of $\tilde{\mu}$ and the domain of definition is $\mathbb{R}^2 \times \{z \in (0,1)\} \times \{t > 0\}$.

For equations (10) the boundary conditions are that (u_i, π, θ) satisfies a plane tiling periodicity in x and y commensurate with the form of periodic cells (typically hexagonal shaped) and on the planes $z = 0, 1$,

$$
w = 0, \quad z = 0, 1; \qquad \theta = 0, \quad z = 0, 1. \tag{15}
$$

We shall also consider the case where the upper boundary is such that the pressure is constant there at the ambient atmospheric pressure p_a, and then the boundary conditions (15) are replaced by

$$
w = 0, \quad z = 0; \qquad \frac{\partial w}{\partial z} = 0, \quad z = 1; \qquad \theta = 0, \quad z = 0, 1. \tag{16}
$$

We only consider equations (16) for the Darcy isotropic case. From equation $(10)_1$ applied on the boundary $z = 1$, $\pi = 0$ when $z = 1$, and this yields u, v zero there, and so from the equation of continuity $w_z = 0$ when $z = 1$. This case is referred by Barletta et al. [44] as corresponding to a perfectly permeable upper boundary. For the non - penetrative convection situation boundary conditions (16) are analysed in detail by Barletta et al. [44], by taking $a_1 = a_2 = b_1 = 0$, $b_2 = \infty$, in their notation. They analyse this class of solutions in section 4.2.4 of their paper and the Rayleigh number against wavenumber curve is given in their Fig. 5 (lower frame) with $a_1 = 0$.

For the Brinkman perturbation equations (14) the boundary conditions are again periodicity in the (x, y) plane and on the boundaries $z = 0, 1$,

$$
u_i = 0, \quad z = 0, 1; \qquad \theta = 0, \quad z = 0, 1. \tag{17}
$$

To find the critical Rayleigh number, wavenumber, and associated eigenfunction, we discard the $Pr\theta^2$ terms and take curlcurl of each of equations $(10)_1$, $(13)_1$, $(14)_1$. We then look for a normal mode solution of form

$$
w = e^{\sigma t}W(z)h(x, y), \qquad \theta = e^{\sigma t}\Theta(z)h(x, y),
$$

where $h(x, y)$ is a plane tiling function, which satisfies $\Delta^* h = -a^2 h$, for a wavenumber a where Δ^* is the horizontal Laplacian, cf. [29, page 51]. This results in having to solve the system of equations

$$\begin{aligned} &(D^2 - a^2)W - 2R(\xi - z)a^2\Theta = 0, \\ &(D^2 - a^2)\Theta - RW = \sigma\Theta, \end{aligned} \tag{18}$$

in the isotropic Darcy case,

$$\begin{aligned} &(D^2 - a^2\ell^2)W - 2R(\xi - z)a^2\Theta = 0, \\ &(D^2 - a^2)\Theta - RW = \sigma\Theta, \end{aligned} \tag{19}$$

in the horizontally isotropic Darcy case, and

$$\begin{aligned} &(D^2 - a^2\ell^2)W - B(D^2 - a^2)^2 W - 2R(\xi - z)a^2\Theta = 0, \\ &(D^2 - a^2)\Theta - RW = \sigma\Theta, \end{aligned} \tag{20}$$

in the horizontally isotropic Brinkman case, where $D = d/dz$ and $z \in (0, 1)$.

The boundary conditions for (18) and (19) are

$$W = 0, \quad z = 0, 1; \qquad \Theta = 0, \quad z = 0, 1; \tag{21}$$

or for the constant pressure case

$$W = 0, \quad z = 0; \qquad DW = 0, \quad z = 1; \qquad \Theta = 0, \quad z = 0, 1; \tag{22}$$

and for (20) for two fixed surfaces

$$W = DW = 0, \quad z = 0, 1; \qquad \Theta = 0, \quad z = 0, 1. \tag{23}$$

5 Global nonlinear stability

For any of the systems of equations (10), (13), or (14), a standard energy stability analysis will not lead to global nonlinear stability due to the presence of the quadratic term $Pr\theta^2 k_i$. Instead, we may employ an energy function which has a weight, of form

$$E(t) = \frac{Pr}{2}\int_V (\zeta - 2z)\theta^2 dx, \tag{24}$$

where $\zeta > 2$ is a constant at our disposal and V is a period cell for the solution, cf. [29, pages 342–343]. When dE/dt is calculated the weight $\zeta - 2z$ gives rise to a term of form $-w\theta^2$ and this cancels out with the analogous term which arises from the momentum equation. Thus, the energy equation which arises contains only quadratic terms which then lead to unconditional (global) nonlinear stability. This leads to an energy equation of form, in the Darcy situation,

$$\frac{dE}{dt} = RI - D, \tag{25}$$

where the dissipation D and the production term I are given by

$$I = -\int_V (2\xi + \zeta - 4z) w\theta \, dx \,,$$

and

$$D = \int_V D_{ij} u_i u_j dx + \int_V (\zeta - 2z) |\nabla\theta|^2 dx.$$

A global nonlinear stability analysis may be developed from (25) as follows

$$\frac{dE}{dt} \leq -D\left(\frac{R}{R_E} - 1\right), \tag{26}$$

where

$$\frac{1}{R_E} = \max_H \frac{I}{D}\,, \tag{27}$$

with $H = \{u_i \in L^2(V), \theta \in H^1(V)\}$ with (x, y) periodicity, being the space of admissible solutions. One has then to calculate the Euler-Lagrange equations from (27) and solve these for the critical value of R_E. This calculation is similar to that done for the linear instability problem in Sect. 7 of this paper. We do not present numerical results for this calculation here since we are primarily interested in the effects of anisotropy and boundary conditions upon penetrative convection. However, the numerical results follow those of Straughan and Walker [16] on a different problem and show that the nonlinear stability threshold is close to the linear instability one for T_U values not exceeding 8 °C.Veronis [2] shows that sub-critical instabilities are possible in the pure fluid penetrative convection problem and so we do not expect coincidence of the energy stability and linear instability Rayleigh number values, especially for T_U larger, where in Sect. 7 we find multi-cellular structures form.

6 Numerical method

To solve equations (18), (19), (20) with boundary conditions (21), (22), (23) numerically we employ a D^2 Chebyshev tau method, as described in Dongarra et al. [62]. We treat σ as the eigenvalue and recast each system into a generalized matrix eigenvalue problem of form

$$A\mathbf{x} = \sigma B\mathbf{x}, \tag{28}$$

where

$$\mathbf{x} = (W_0, \cdots, W_N, \Theta_0, \cdots, \Theta_N),$$

for the Darcy cases with

$$W = \sum_{i=0}^{N} W_i T_i(z), \qquad \Theta = \sum_{i=0}^{N} \Theta_i T_i(z), \tag{29}$$

where $T_i(z)$ are Chebyshev polynomials. For the Brinkman case we introduce a variable χ by $\chi = (D^2 - a^2)W$ and then we still have a system like (28) to solve but now

$$\mathbf{x} = (W_0, \cdots, W_N, \chi_0, \cdots, \chi_N, \Theta_0, \cdots, \Theta_N). \tag{30}$$

The boundary conditions (21) and (23) are inserted as rows $N-1, N, 2N-1, 2N$ for the Darcy problem and rows $N-1, N, 2N-1, 2N, 3N-1, 3N$ for the Brinkman problem. For these cases the resulting generalized matrix eigenvalue problem was solved by the QZ algorithm of Moler and Stewart [63]. The eigenfunctions $W(z)$ are calculated from the eigenvalues W_i as in (29) or (30).

For the constant pressure boundary condition (22) we found significant problems with the production of spurious eigenvalues if we used the method of writing in the boundary conditions as rows of the matrices. To overcome this it was necessary to use the discrete form of the boundary conditions to remove variables W_{N+1} and W_{N+2} and in this manner to incorporate the boundary conditions into all rows of the matrices. The relevant expressions are given by (2.15) and (2.16) of Payne and Straughan [64] taking their variable $\mathcal{A} = 0$. In our case the appropriate conditions are

$$\begin{aligned} W_{N+1} &= -\sum_{i=0}^{N} \left(\frac{i^2 + (-1)^i (N+2)^2}{2N^2 + 6N + 5} \right) W_i, \\ W_{N+2} &= \sum_{i=0}^{N} \left(\frac{-i^2 + (-1)^i (N+1)^2}{2N^2 + 6N + 5} \right) W_i. \end{aligned}$$

The conditions on W_{N+1} and W_{N+2} may be found by using the relations $T_n(\pm 1) = (\pm 1)^n$, $T_n'(\pm 1) = n^2 (\pm 1)^{n-1}$. The domain (0,1) is transformed to the Chebyshev domain (-1,1) by $z = 2\hat{z} - 1$ and then the boundary conditions $W = 0,\ z = 0$ and $DW = 0,\ z = 1$ are

$$\begin{aligned} W_0 - W_1 + W_2 - \cdots + W_{N+1} - W_{N+2} &= 0, \\ W_1 + 4W_2 + \cdots + (N+1)^2 W_{N+1} + (N+2)^2 W_{N+2} &= 0. \end{aligned}$$

The expressions for W_{N+1} and W_{N+2} are obtained by elimination from these two equations.

We put $\sigma = \sigma_r + \sigma_1$, $\sigma_r, \sigma_1 \in \mathbb{R}$, and the secant method is employed to locate where $\sigma_r = 0$. We then minimize the value of Ra so found in a^2 to yield the critical values of Ra and a. It is of interest to note that for all the cases we have performed we found $\sigma_1 = 0$ at criticality. While we do not have a rigorous proof that $\sigma \in \mathbb{R}$, i.e. that the principle of exchange of stabilties holds, it is certainly found numerically in all the results shown here.

7 Numerical results

Numerical results for critical wavenumbers, a, and Rayleigh numbers, Ra, are presented in tables 1 - 6. The W eigenfunctions associated to the critical values of a and Ra are displayed in Figs. 1, 2, 3, 4.

Tables 1, 2, 3 concentrate on isotropic theory and concern, respectively, the Darcy model with $W = 0$ on the upper surface, the Darcy model with constant pressure on the upper surface, and the Brinkman model for two fixed surfaces. The corresponding eigenfunctions are presented in Figs. 1, 2, 3. For the Brinkman model the results are presented in terms of a Rayleigh number

$$Ra = \xi^5 R^2,$$

so that the depth of the destabilizing layer is reflected in that case.

Table 1 Critical wavenumber, a, critical Rayleigh number, $Ra = \xi^3 R^2$, number of convection cells (if any, denoted by change of sign in W), for varying upper temperature, T_U. Isotropic Darcy theory with $W = 0$ at $z = 1$

T_U	a	Ra	$W < 0$ (no. cells)
4	3.20	38.540	No
6	3.51	29.338	No
8	4.675	29.461	Yes (2 cells)
10	5.88	29.502	Yes
12	7.05	29.501	Yes (3 cells)
14	8.23	29.501	Yes
16	9.40	29.501	Yes (4 cells)

Table 2 Critical wavenumber, a, critical Rayleigh number, $Ra = \xi^3 R^2$, number of convection cells (if any, denoted by change of sign in W), for varying upper temperature, T_U. Isotropic Darcy theory with $DW = 0$ at $z = 1$

T_U	a	Ra	$W < 0$ (no. cells)
4	2.45	30.933	No
6	3.25	28.645	No
8	4.71	29.523	Yes (2 cells)
10	5.80	29.500	Yes
12	7.05	29.502	Yes (3 cells)
14	8.23	29.501	Yes
16	9.40	29.501	Yes (4 cells)

Table 3 Critical wavenumber, a, critical Rayleigh number, $Ra = \xi^5 R^2$, number of convection cells (if any, denoted by change of sign in W), for varying upper temperature, T_U. Isotropic Brinkman theory with $W = 0$ at $z = 1$

T_U	a	Ra	$W < 0$ (no. cells)
4	3.13	1738.830	No
6	3.20	649.256	No
8	4.01	593.110	Yes (2 cells)
10	5.11	596.476	Yes
12	6.11	593.689	Yes (3 cells)
14	7.12	592.509	Yes
16	8.14	591.757	Yes (4 cells)

Table 1 shows that the critical wavenumber increases as T_U increases, which is equivalent to the aspect ratio of the convection cell (width/depth) for constant depth decreasing. We do not witness counter cells for $T_U = 4, 6$, but there is one counter cell when $T_U = 8$, but the aspect ratio is less. When $T_U = 12$ we find 3 cells and when $T_U = 16$ there are 4 cells, with the cell width being approximately one third of that when $T_U = 4$. The pattern of cell formation is repeated in Tables 2, 3, for Darcy theory with a constant pressure boundary condition, and Brinkman theory, respectively. As T_U increases the critical Ra values tend to a constant which is different in the Brinkman case to the two Darcy theories. The value of Ra as T_U increases is the same for both of the Darcy theories and the eigenfunctions are very similar which suggests that for $T_U \geq 12$ the upper boundary condition on W is less relevant. The narrowness of the convection cells and greater temperature variation appears to be more influential to cell formation.

The transition value from one cell to two cells varies for each model. For the Darcy theory with $W = 0$ on the upper boundary we find two cells are present when $T_U = 6.5$, whereas with a constant pressure boundary condition $T_U = 6.6$. For the Brinkman theory with $B = 1$ or 10 we find two cells when $T_U = 7.2$. When $B = 0.1$ the relevant value is $T_U = 7.1$ and when $B = 0.01$, $T_U = 6.8$.

The eigenfunctions for Darcy theory with $W = 0$ on the upper surface or for a constant pressure boundary condition are very close for $T_U = 8, 12, 16$, apart from near to the upper surface $z = 1$. When $T_U = 8$ the strength of the counter cell is 0.0877 for the constant pressure boundary condition whereas it is 0.0718 for $W = 0$ at $z = 1$. When $T_U = 12$ the second cells have the same strength with the strength of the third cell being 1.6 times greater for the constant pressure case. When $T_U = 16$ the strengths of the second and third cells are the same for $W = 0$ or constant pressure boundary conditions, but the fourth cell is approximately 1/3 times stronger for the constant pressure boundary condition.

There is a greater variation of strength in the Brinkman case where the Laplacian term plays a strong role. The second counter cells for $T_U = 12, 16$ are much stronger for the Brinkman theory as is witnessed in Fig. 3.

In Table 4 we show critical wavenumber and Rayleigh number values for the Darcy problem with $T_U = 6$ and $W = 0$ on the upper boundary, the corresponding $W(z)$ eigenfunction behaviour is seen in Fig. 4. The effect of anisotropy is observed. This was also investigated by Carr and Putter [20], but for different values. The horizontal isotropy has a strong effect upon critical values and, indeed, upon convection cell structure. As ℓ^2 increases a decreases which means the aspect ratio increases and the cells become wider. Also, for $\ell^2 = 10$ we see a second cell has formed. This is in complete agreement with the observations by Musman [17] for penetrative convection in a layer of pure water, who writes,... "*The most important penetration of convective motions takes place in the form of nearly horizontal motions in the lowest part of the stable region, corresponding to the upper part of the principal cell.*" For ℓ^2 large the horizontal permeability is significantly larger than the vertical one and this will assist horizontal motion and so extra cells will be expected physically for larger values of ℓ^2.

In Table 5 critical Ra and a values are given for the Darcy theories and they are compared with the Brinkman values over a similar T_U range. The variation of critical wavenumbers and Rayleigh numbers as ℓ^2 changes for the Brinkman theory is noticeable. When $T_U = 6.8$ we see that ℓ^2 has to be very large for a counter cell to form.

The effect of the variation of the Brinkman parameter B is displayed in Table 6. It is noted that the counter cell occurence does not appear to be influenced much by B variation, e.g. for $T_U = 7.1$, $B = 1, 10$ indicates only one principal cell, and when $T_U = 7.2$ a counter cell appears for $B = 0.1, 1$ and 10. The effect of variation of T_U for $B = 0.01$ is given and a counter cell is observed when $T_U = 6.8$.

Table 4 Critical wavenumber, a, critical Rayleigh number, $Ra = \xi^3 R^2$, whether W changes sign in (0, 1), for fixed upper temperature, $T_U = 6$, with varying anisotropy parameter ℓ^2. Darcy theory with $W = 0$ at $z = 1$

ℓ^2	a	Ra	$W < 0$
10	2.01	124.944	Yes
2	2.96	42.675	No
1	3.51	29.338	No
0.5	4.18	21.337	No
0.1	6.35	12.494	No

Table 5 Critical wavenumber, a, critical Rayleigh number, $Ra = \xi^3 R^2$, whether W changes sign in (0, 1), for various upper temperatures, with varying anisotropy parameter ℓ^2, for Darcy theory, Darcy theory with constant pressure boundary condition, or Brinkman theory as indicated. For the Darcy theories $Ra = \xi^3 R^2$, whereas for the Brinkman theory $Ra = \xi^5 R^2$

Theory	T_U	ℓ^2	a	Ra	$W < 0$
Darcy	6.6	1	3.78	29.169	Yes
Constant Pressure	6.6	1	3.76	29.237	Yes
Darcy	6.7	1	3.83	29.183	Yes
Constant Pressure	6.7	1	3.84	29.298	Yes
Brinkman $B = 1$	6.7	1	3.32	580.678	No
Brinkman $B = 1$	6.0	10	3.11	712.821	No
Brinkman $B = 1$	6.0	100	2.57	1271.420	No
Brinkman $B = 1$	6.8	10	3.26	630.591	No
Brinkman $B = 1$	6.8	100	2.78	1095.691	Yes

Table 6 Critical wavenumber, a, critical Rayleigh number, $Ra = \xi^5 R^2$, whether W changes sign in (0, 1), for various upper temperatures, with varying Brinkman parameter B

B	T_U	a	Ra	$W < 0$
0.07	7.1	3.56	51.283	Yes
0.09	7.1	3.54	62.564	Yes
0.1	7.1	3.53	68.196	Yes
1	7.1	3.46	573.094	No
10	7.1	3.45	5619.834	No
0.1	7.2	3.58	68.035	Yes
1	7.2	3.50	573.799	Yes
10	7.2	3.49	5629.156	Yes
0.1	6.5	3.33	71.582	No
0.1	7.0	3.49	68.447	No
0.01	6.5	3.57	18.681	No
0.01	6.6	3.61	18.290	No
0.01	6.7	3.65	17.929	No
0.01	6.8	3.70	17.597	Yes
0.01	7.0	3.80	17.001	Yes

Table 7 shows how the critical Rayleigh number varies with the upper surface temperature T_U (which is equivalent to varying ξ) for fixed values of the Brinkman number, 0.1 and 1. Figures 5 and 6 display this variation. The behaviour is similar in each figure although the scale is different. Tables 8, 9, 10 show how the critical Rayleigh number varies with the Brinkman number B for fixed values of T_U and anisotropy ℓ^2. These results are displayed graphically in Fig. 7. For $\ell^2 = 1$ or 10 we find that the graphs of $log_{10} Ra$ against $log_{10} B$ are almost straight lines, thus displaying nearly linear variation. For $\ell^2 = 100$ where the horizontal permeability is much greater than the vertical one this is not true for small B although as B increases the curves approach a linear relationship. This is understandable since for B small the Darcy term is dominating via the strong horizontal permeability.

Table 7 Critical wavenumber, a, critical Rayleigh number, $Ra = \xi^5 R^2$, with varying T_U (alternatively varying $\xi \equiv 4/T_U$) for $B = 0.1, 1$. Brinkman theory with $\ell^2 = 1$

T_U	ξ	B	a	Ra	B	a	Ra
4	1	0.1	3.16	213.181	1	3.13	1738.830
4.25	0.9412	0.1	3.17	177.989	1	3.13	1452.232
4.5	0.8889	0.1	3.17	151.246	1	3.14	1234.526
4.75	0.8421	0.1	3.18	130.665	1	3.14	1067.076
5	0.8	0.1	3.18	114.676	1	3.15	937.119
5.5	0.7273	0.1	3.21	92.419	1	3.17	756.762
6	0.6667	0.1	3.25	79.004	1	3.20	649.256
6.5	0.6154	0.1	3.33	71.582	1	3.27	592.240
7	0.5714	0.1	3.49	68.447	1	3.42	573.302
8	0.5	0.1	4.08	68.040	1	4.01	593.110
9	0.4444	0.1	4.68	66.924	1	4.62	600.961
10	0.4	0.1	5.16	65.220	1	5.11	596.476
11	0.3636	0.1	5.65	64.064	1	5.60	594.323
12	0.3333	0.1	6.16	63.266	1	6.11	593.689

Table 8 Critical wavenumber, a, critical Rayleigh number, $Ra = \xi^5 R^2$, with varying B, $T_U = 8$, ($\xi = 0.5$). Brinkman theory, with horizontally isotropic Darcy coefficient

B	$log_{10}B$	ℓ^2	a	Ra	$log_{10}Ra$	ℓ^2	a	Ra	$log_{10}Ra$
0.1	−1	1	4.08	68.04	1.8328	10	3.65	104.86	2.0206
0.2	−.69897	1	4.04	126.46	2.1019	10	3.79	165.63	2.2191
0.5	−.301	1	4.02	301.48	2.4793	10	3.90	342.77	2.5350
1	0	1	4.01	593.11	2.7731	10	3.95	635.31	2.8030
3.2	.50515	1	4.00	1876.18	3.2733	10	3.98	1919.10	3.2831
10	1	1	4.00	5841.98	3.7666	10	3.99	5885.14	3.7698
32	1.50515	1	4.00	18672.52	4.2712	10	4.00	18715.76	4.2722
100	2	1	4.00	58330.52	4.7659	10	4.00	58373.78	4.7662

Table 9 Critical wavenumber, a, critical Rayleigh number, $Ra = \xi^5 R^2$, with varying B, $T_U = 6$, ($\xi = 0.6667$). Brinkman theory, with horizontally isotropic Darcy coefficient

B	$log_{10}B$	ℓ^2	a	Ra	$log_{10}Ra$	ℓ^2	a	Ra	$log_{10}Ra$
0.1	-1	1	3.25	79.00	1.8976	100	1.76	559.47	2.7478
0.2	-.69897	1	3.23	142.43	2.1536	100	1.97	663.33	2.8217
0.5	-.301	1	3.21	332.51	2.5218	100	2.31	912.43	2.9602
1	0	1	3.20	649.26	2.8124	100	2.57	1271.42	3.1043
3.2	.50515	1	3.20	2042.87	3.3103	100	2.92	2716.52	3.4340
10	1	1	3.20	6350.36	3.8028	100	3.09	7048.31	3.8481
32	1.50515	1	3.20	20286.35	4.3072	100	3.16	20993.64	4.3221
100	2	1	3.20	63361.24	4.8018	100	3.19	64071.60	4.8067

Table 10 Critical wavenumber, a, critical Rayleigh number, $Ra = \xi^5 R^2$, with varying B, $T_U = 4$, ($\xi = 1$). Brinkman theory, with horizontally isotropic Darcy coefficient

B	$log_{10}B$	ℓ^2	a	Ra	$log_{10}Ra$	ℓ^2	a	Ra	$log_{10}Ra$
0.1	-1	1	3.16	213.18	2.3287	100	1.59	1582.88	3.1994
0.2	-.69897	1	3.15	382.78	2.5830	100	1.82	1849.65	3.2671
0.5	-.301	1	3.13	891.33	2.9500	100	2.17	2505.11	3.3988
1	0	1	3.13	1738.83	3.2403	100	2.45	3460.17	3.5391
3.2	.50515	1	3.13	5467.74	3.7378	100	2.82	7321.66	3.8646
10	1	1	3.13	16993.43	4.2303	100	3.01	18910.14	4.2767
32	1.50515	1	3.13	54282.40	4.7347	100	3.09	56223.06	4.7499
100	2	1	3.13	169539.21	5.2293	100	3.11	171488.07	5.2342

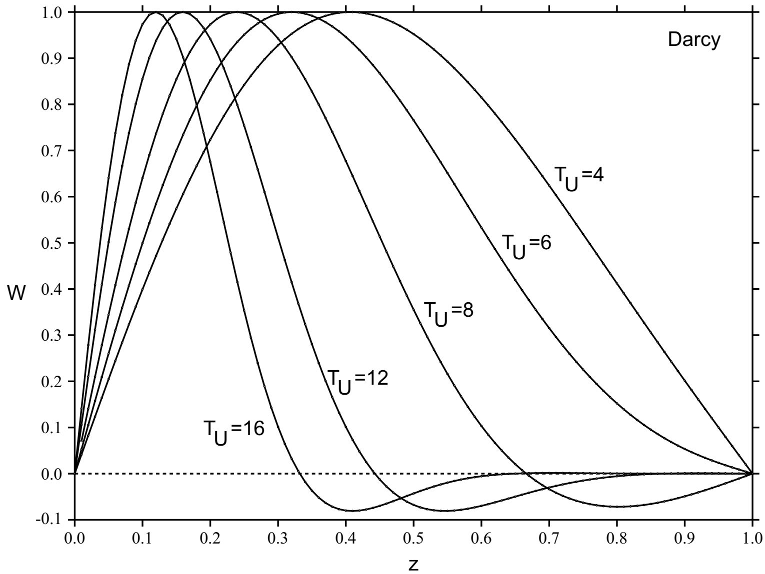

Fig. 1 Graph of W against T_U for Darcy isotropic theory with $W = 0$ at $z = 1$. The values of T_U are marked on the graph

8 Conclusions

Penetrative convection in a horizontal layer of water saturated porous material has been studied. The problem is much richer in a porous material than in the pure fluid case since one must consider the appropriate porous medium model, the porous medium may be strongly anisotropic, and if a Brinkman theory is employed the strength of this effect has to be investigated.

We have analysed two porous medium theories, that of Darcy and also that of Brinkman. We have also allowed for different boundary conditions on the velocity on the upper surface of the layer. We have shown that anisotropy and the Brinkman effect may alter the critical wave and Rayleigh numbers substantially, and may also affect the structure of

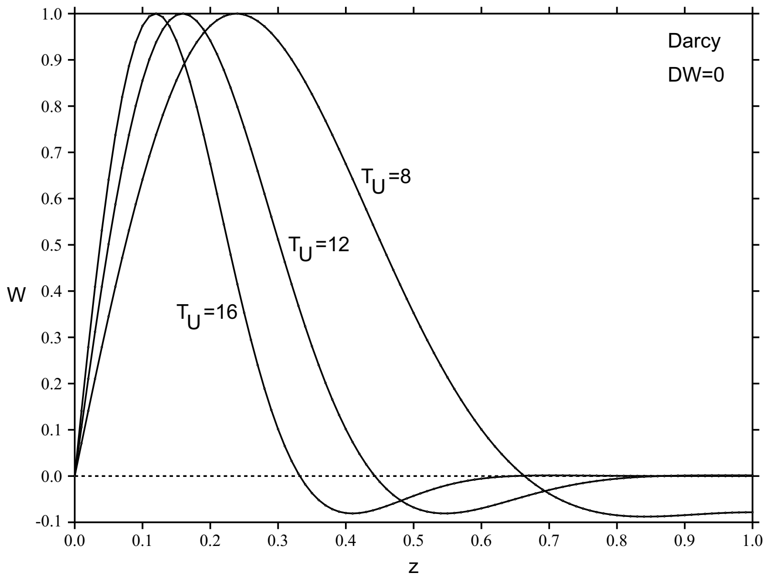

Fig. 2 Graph of W against T_U for Darcy isotropic theory with $DW = 0$ at $z = 1$. The values of T_U are marked on the graph

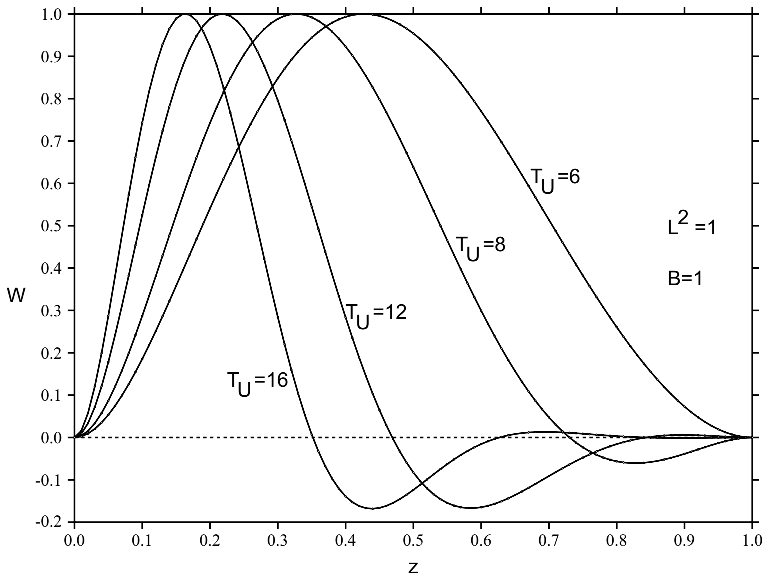

Fig. 3 Graph of W against T_U for Brinkman isotropic theory with two fixed surfaces. The values of T_U are marked on the graph

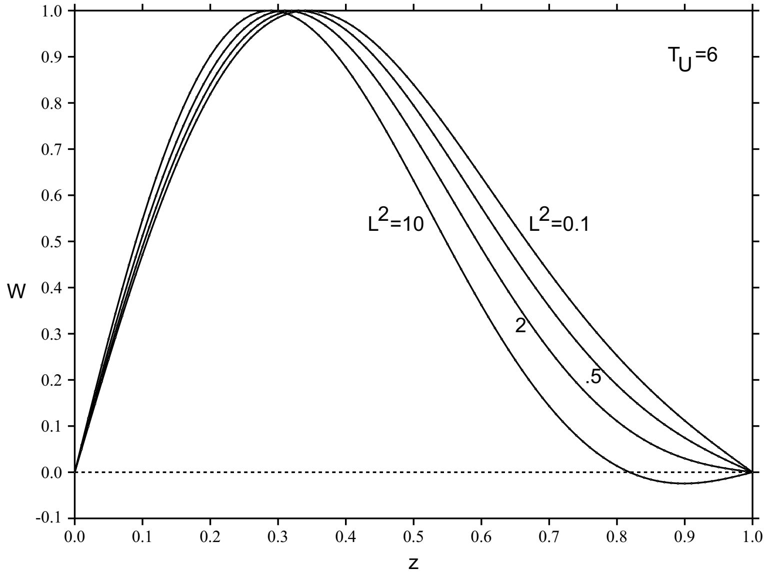

Fig. 4 Graph of W against ℓ^2 for Darcy isotropic theory with $W = 0$ at $z = 1$. The upper temperature is fixed at $T_U = 6$ °C. The values of ℓ^2 are 10, 2, 0.5 and 0.1, with $\ell^2 = 1$ being in figure 1

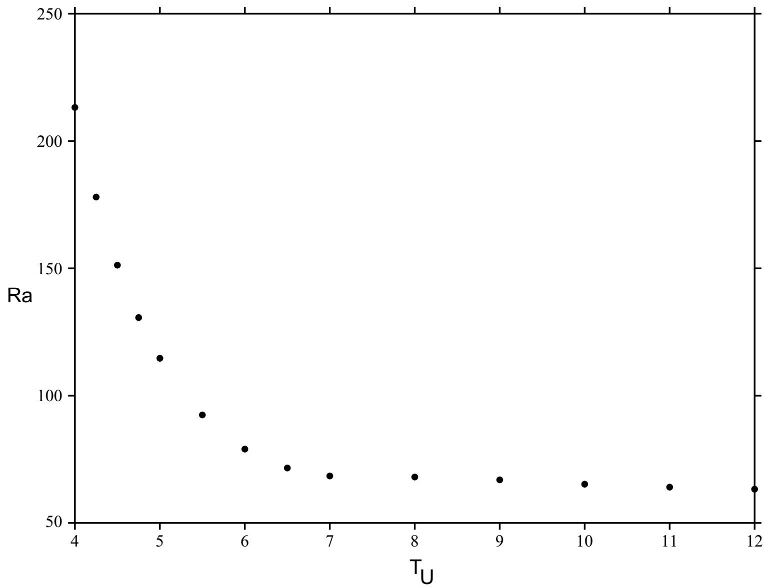

Fig. 5 Graph of Ra against T_U for Brinkman isotropic theory with two fixed surfaces. The Brinkman parameter has value $B = 0.1$

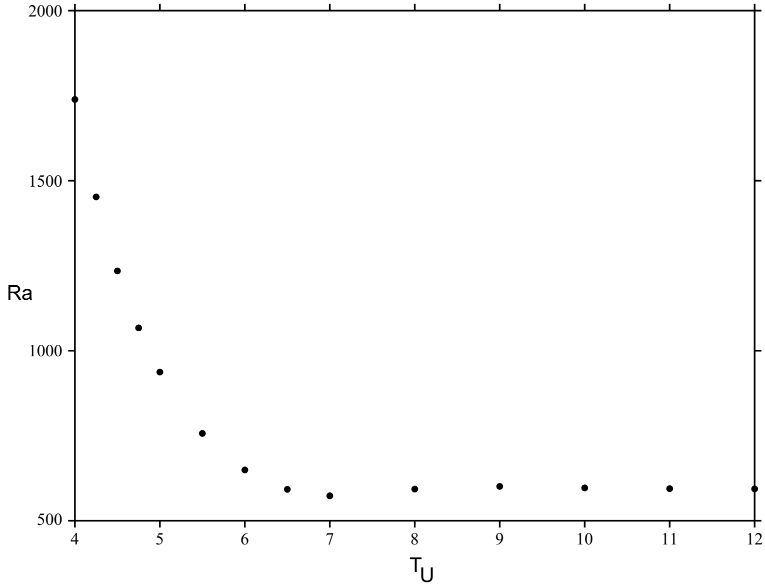

Fig. 6 Graph of Ra against T_U for Brinkman isotropic theory with two fixed surfaces. The Brinkman parameter has value $B = 1$

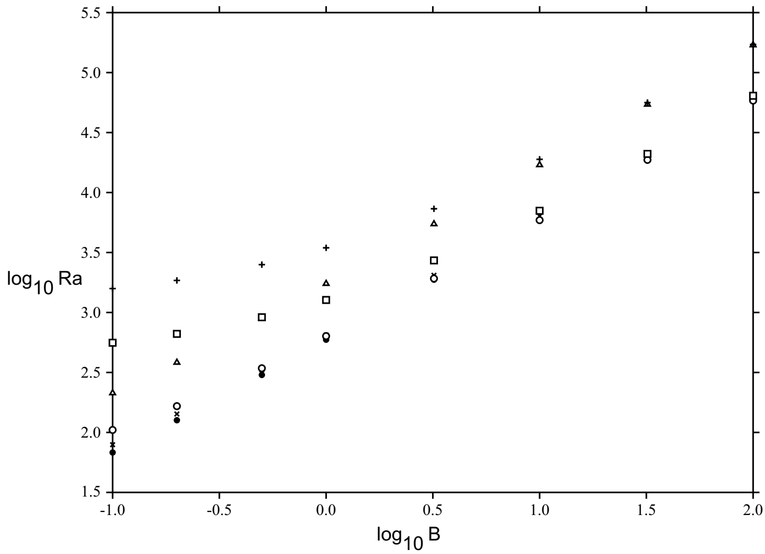

Fig. 7 Graph of $log_{10} Ra$ against $log_{10} B$ for Brinkman theory with two fixed surfaces. The solid circle is for $T_U = 8$, $(\xi = 0.5)$, $\ell^2 = 1$, the cross is for $T_U = 6$, $(\xi = 0.6667)$, $\ell^2 = 1$, the open circle is for $T_U = 8$, $(\xi = 0.5)$, $\ell^2 = 10$, the triangle is for $T_U = 4$, $(\xi = 1)$, $\ell^2 = 1$, the open square is for $T_U = 6$, $(\xi = 0.6667)$, $\ell^2 = 100$. the plus sign is for $T_U = 4$, $(\xi = 1)$, $\ell^2 = 100$

convection cell formation. For the Darcy theory the upper boundary condition of zero vertical velocity or constant pressure is important when the upper temperature is less than 8 °C, but the difference in the effect of the boundary conditions becomes much less when the upper temperature takes the values of 12 °C or 16 °C.

Acknowledgements I am indebted to two anonymous referees for their critiscism and constructive suggestions. This has led to substantial improvement in the manuscript.

Author Contributions This work was performed 100 per cent by B. Straughan, who also completely wrote the article.

Funding This work was supported by the Leverhulme Trust, grant number EM-2019-022/9.

Declarations

Conflict of interest There are no conflicts of interest.

References

1. Straughan B (2015) Convection with local thermal non-equilibrium and microfluidic effects, volume32 of Advances in Mechanics and Mathematics Series. Springer, Cham
2. Veronis G (1963) Penetrative convection. Astrophys J 137:641–663
3. Dietrich W, Wicht J (2018) Penetrative convection in partly stratified rapidly rotating spherical shells. Front Earth Sci. https://doi.org/10.3389/feart.2018.00189
4. Vanden Berg AP, Yuen DA, Beebe GL, Christiansen MD (2010) The dynamical impact of electronic thermal conductivity on deep mantle convection of exosolar planets. Phys Earth Planet Inter 178:136–154
5. Berlengiero M, Emanuel KA, von Hardenberg J, Provenzale A, Spiegel EA (2012) Internally cooled convection: a fillip for Philip. Commun Nonlinear Sci Numer Simul 17:1998–2007
6. Fernando HJS (1987) The formation of a layered structure when a stable salinity gradient is heated from below. J Fluid Mech 182:525–541
7. Pol SU, Fernando HJS (2017) Penetrative convection in slender cylinders. Environmental Fluid Mech 17:799–814
8. Imamura T, Higuchi T, Maejima M, Takagi Y, Sugimoto N, Ikeda K, Ando H (2014) Inverse insolation dependence of Venus' cloud - level convection. Icarus 228:181–188
9. Kaminski E, Chenet AL, Jaupart C, Courtillot V (2011) Rise of volcanic plumes to the stratosphere aided by penetrative convection above large lava flows. Earth Planetary Sci Lett 301:171–178
10. Kirillov SA, Dmitrenko IA, Hölemann JA, Kassens H, Bloshkina E (2013) The penetrative mixing in the Laptev sea coastal polyna pynocline layer. Cont Shelf Res 63:34–42
11. Machado LAT, Lima WFA, Pinto O, Morales CA (2009) Relationship between cloud-to-ground discharge and penetrative clouds: a multi-channel satellite application. Atmos Res 93:304–309
12. Mharzi M, Daguenet M, Daoudi S (2000) Thermosolutal natural convection in a vertically layered fluid - porous medium heated from the side. Energy Convers Manage 41:1065–1090
13. Prudhomme M, Jasmin S (2006) Inverse solution for a biochemical heat source in a porous medium in the presence of natural convection. Chem Eng Sci 61:1667–1675

14. Tikhomolov E (2005) Large - scale vortical flows and penetrative convection in the sun. Nucl Phys A 758:709c–712c
15. George JH, Gunn RD, Straughan B (1989) Patterned ground formation and penetrative convection in porous media. Geophys Astrophys Fluid Dyn 46:135–158
16. Straughan B, Walker DW (1996) Anisotropic porous penetrative convection. Proc R Soc London A 452:97–115
17. Musman S (1968) Penetrative convection. J Fluid Mech 31:343–360
18. Carr M (2003) Convection in fluid and porous media. PhD thesis, University of Durham,
19. Carr M (2004) Penetrative convection in a superposed porous - medium - fluid layer via internal heating. J Fluid Mech 509:305–329
20. Carr M, dePutter S (2003) Penetrative convection in a horizontally isotropic layer. Cont Mech Thermodyn 15:33–43
21. Carr M, Straughan B (2003) Penetrative convection in a fluid overlying a porous layer. Adv Water Resour 26:263–276
22. Harfash AJ (2014) Structural stability for two convection models in a reacting fluid with magnetic field effect. Ann Henri Poincaré 15:2441–2465
23. Harfash AJ (2016) Resonant penetrative convection in porous media with an internal heat source/sink effect. Appl Math Comp 281:323–342
24. Krishnamurti R (1997) Convection induced by selective absorption of radiation: a laboratory model of conditional instability. Dyn Atmos Oceans 27:367–382
25. Larson VE (2001) The effects of thermal radiation on dry convective instability. Dyn Atmos Oceans 34:45–71
26. Straughan B (2004) Resonant porous penetrative convection. Proc R Soc London A 460:2913–2927
27. Straughan B (2012) Triply resonant penetrative convection. Proc R Soc London A 468:3804–3823
28. Straughan B (2016) Importance of Darcy or Brinkman laws upon resonance in thermal convection. Ricerche Matem 65:349–362
29. Straughan B (2004) The energy method, stability, and nonlinear convection, volume91 of Appl Math Sci, 2nd edn. Springer, New York
30. Straughan B (2008) Stability, and wave motion in porous media. Springer, New York
31. Capone F, Gentile M, Gianfrani JA (2021) Optimal stability thresholds in rotating fully anisotropic porous medium with LTNE. Transp Porous Media 139:185–202
32. Capone F, Gentile M, Massa G (2021) The onset of thermal convection in anisotropic and rotating bidisperse porous media. ZAMP 72:169
33. Capone F, DeLuca R, Gentile M (2020) Thermal convection in rotating anisotropic porous layers. Mech Res Comm 110:103601
34. Capone F, Gentile M, Hill AA (2012) Convection problems in anisotropic porous media with non - homogeneous porosity and thermal diffusivity. Acta Appl Math 122:85–91
35. Capone F, Gentile M, Hill AA (2011) Double diffusive penetrative convection simulated via internal heating in an anisotropic porous layer with throughflow. Int J Heat Mass Transfer 54:1622–1626
36. Hemanthkumar C, Shivakumara IS, Shankar BM, Pallavi G (2021) Exploration of anisotropy on nonlinear stability of thermohaline viscoelastic porous convection. Int Comm Heat Mass Transfer 126:105427
37. Straughan B (2018) Horizontally isotropic bidispersive thermal convection. Proc R Soc London A 474:20180018
38. Straughan B (2019) Anisotropic bidispersive convection. Proc R Soc London A 475:20190206
39. Fang Y, Ouyang L, Zhang T, Wang C, Lu B, Sun W (2020) Optimizing bifurcated channels within an anisotropic scaffold for engineering vascularized oriented tissues. Adv Healthc Mater 9:2000782
40. Mirbod P, Wu Z, Ahmadi G (2017) Laminar flow drag reduction on soft porous media. Nat Sci Rep 7:17263
41. Rees DAS (2002) The onset of Darcy - Brinkman convection in a porous layer: an asymptotic analysis. Int J Heat Mass Transfer 45:2213–2220
42. Gentile M, Straughan B (2020) Bidispersive thermal convection with relatively large macropores. J Fluid Mech 898:A14
43. Wu Z, Mirbod P (2019) Instability analysis of the flow between two parallel plates where the bottom one is coated with porous media. Adv Water Resour 130:221–228
44. Barletta A, Tyvand PA, Nygard HS (2015) Onset of thermal convection in a porous layer with mixed boundary conditions. J Eng Math 91:105–120
45. Barletta A (2012) Thermal instability in a horizontal porous channel with horizontal through flow and symmetric wall heat fluxes. Transp Porous Media 92:419–437

46. Barletta A, Celli M, Nield DA (2010) Unstably stratified Darcy flow with impressed horizontal temperature gradient, viscous dissipation and asymmetric thermal boundary conditions. Int J Heat Mass Transfer 53:1621–1627
47. Barletta A, Celli M (2018) The Horton - Rogers - Lapwood problem for an inclined porous layer with permeable boundaries. Proc R Soc London A 474:20180021
48. Barletta A, Rees DAS (2012) Local thermal non-equilibrium effects in the Darcy - Bénard instability with isoflux boundary conditions. Int J Heat Mass Transfer 55:384–394
49. Celli M, Kuznetsov AV (2018) A new hydrodynamic boundary condition simulating the effect of rough boundaries on the onset of Rayleigh - Bénard convection. Int J Heat Mass Transfer 116:581–586
50. Mohammad AV, Rees DAS (2017) The effect of conducting boundaries on the onset of convection in a porous layer which is heated from below by inclined heating. Trans Por Media 117:189–206
51. Nield DA, Kuznetsov AV (2016) Do isoflux boundary conditions inhibit oscillatory double - diffusive convection. Transp Porous Media 112:609–618
52. Rees DAS, Barletta A (2011) Linear instability of the isoflux Darcy - Bénard problem in an inclined porous layer. Trans Por Media 87:665–678
53. Rees DAS, Mojtabi A (2011) The effect of conducting boundaries on weakly nonlinear Darcy - Bénard convection. Trans Por Media 88:45–63
54. Rees DAS, Mojtabi A (2013) The effect of conducting boundaries on Lapwood - Prats convection. Int J Heat Mass Transfer 65:765–778
55. Brandao PV, Barletta A, Celli M, deAlves LS, Rees DAS (2021) On the stability of the isoflux Darcy - Bénard problem with a generalized basic state. Int J Heat Mass Transfer 177:121538–63
56. Li Y, Zhang S, Lin C (2021) Structural stability for the Brinkman equations interfacing with Darcy equations in a bounded domain. Bound Value Probl. https://doi.org/10.1186/s13661-021-01501-0
57. Liu Y, Xiao S (2018) Structural stability for the Brinkman fluid interfacing with a Darcy fluid in an unbounded domain. Nonlinear Anal Real World Appl 42:308–333
58. Liu Y, Xiao S, Lin YW (2018) Continuous dependence for the Brinkman - Forchheimer fluid interfacing with a Darcy fluid in a bounded domain. Math Comp Simul 150:66–88
59. Li Y, Xiao S, Lin Y (2018) Continuous dependence for the Brinkman - Forchheimer fluid interacting with a Darcy fluid in a bounded domain. Math Comp Simul 150:66–82
60. Li Y, Chen X, Shi J (2021) Structural stability in resonant penetrative convection in a Brinkman - Forchheimer fluid interfacing with a Darcy fluid. Appl Math Optim. https://doi.org/10.1007/s00245-021-09791-7
61. Gentile M, Straughan B (2013) Structural stability in resonant penetrative convection in a Forchheimer porous material. Nonlinear Anal Real World Appl 14:397–401
62. Dongarra JJ, Straughan B, Walker DW (1996) Chebyshev tau - QZ algorithm methods for calculating spectra of hydrodynamic stability problems. Appl Numer Math 22:399–435
63. Moler CB, Stewart GW (1971) An algorithm for the generalized matrix eigenvalue problem $Ax = \lambda Bx$. Univ. Texas at Austin, Technical report
64. Payne LE, Straughan B (2000) A naturally efficient numerical technique for porous convection stability with non - trivial boundary conditions. Int J Numer Anal Geomech 24:815–836